

classified as type M and, when classifying in the blue spectral region, slight ZrO enhancements are easily overlooked, the latter explanation seems likely. To complicate matters further, the number of MS standards is very small and at least some of them have variable abundance class.

From their position in the colour-magnitude diagram, the MS stars are estimated to have masses around $5 M_{\odot}$. Most of the carbon stars in the field investigated by Wood et al. (1983) were found to have pulsational masses around $1 M_{\odot}$. The luminous J-type (^{13}C -

rich) carbon stars (Richer et al. 1979) probably represent higher masses. The J-type carbon stars are known not to have enhanced s-process element abundances while the N-type, non-J, carbon stars have this enhancement. Unfortunately, s-process element abundances are not available for the MS stars but would be very useful in determining the relation between the two groups of carbon stars and the MS stars. This relation is at present not clear, but the MS stars are more massive than the bulk of ordinary N-type carbon stars and may be more closely

related to the luminous J-type carbon stars.

References

- Iben, I.Jr., and Renzini, A.: 1983, *Ann. Rev. Astron. Astrophys.* **21**, 271.
 Keenan, P.C., and Boeshaar, P.C.: 1980, *Astrophys. J. Suppl.* **43**, 379.
 Lloyd Evans, T.: 1983, *Monthly Notices Roy. Astr. Soc.* **204**, 975.
 Richer, H.B., Olander, N., and Westerlund, B.E.: 1979, *Astrophys. J.* **230**, 724.
 Westerlund, B.E., Olander, N., and Hedin, B.: 1981, *Astron. Astrophys. Suppl.* **43**, 272.
 Wood, P.R., Bessell, M.S., and Fox, W.: 1983, *Astrophys. J.* **272**, 99.

HD 187474: the First Results of Surface Magnetic Field Measurements

P. DIDELO, *Observatoire de Strasbourg, France*

1. Introduction

The upper main-sequence chemically peculiar stars (CP, see Preston 1974) were the first non degenerate stars definitely showing magnetic field with large scale structure. The magnetic field usually observed in CP stars is dipolar. More complicated structures are perhaps present, but their contributions are certainly smaller (Landstreet, 1980). As the star rotates, the visible hemisphere changes and magnetic field variations are observed. The magnetic field seems to play an important role in the physical phenomena occurring in the magnetic CP stars (diffusion, blanketing, structure of the atmosphere, . . .), and a better knowledge of it is therefore important for our understanding of the CP phenomenon.

The magnetic field is detected through the splitting of a line into several components: π components are symmetrically displaced around the central wavelength λ_0 , while σ components are displaced to shorter or longer wavelengths. In the most simple case, the line is split into a triplet pattern with three components: one undisplaced π component and two symmetrically displaced σ components. These components are also polarized and their polarizations depend on the magnetic field orientation.

The mean displacement of the σ components from the central wavelength λ_0 is given by:

$$\Delta\lambda = 4.67 \times 10^{-13} z B \lambda_0^2 \quad (1)$$

for wavelength expressed in \AA ; z is the mean Landé factor of the σ component

and B is the magnetic field in gauss. The mean Landé factor of the σ components z is also called effective Landé factor (g_{eff}). It appears immediately that this displacement is very small, of the order of 100 milliangström per kilogauss at 5000\AA for $z = 1$. Generally it is smaller than broadening due to other mechanisms (thermal, collisional broadening), the most important and unavoidable one is the rotational broadening.

The splitting measured in circularly polarized light gives access to the average longitudinal magnetic field, also called "effective" magnetic field (H_{eff}). It is the average on the visible hemisphere of the magnetic field projection on the line of sight. One advantage of this method is that by recording separately the right and left circularly polarized light, small relative displacements of the same line, between the two spectra, can easily be detected. Several different methods of circular polarization measurement across spectral lines have been used to deduce stellar effective magnetic fields (Landstreet, 1980).

The splitting measured in unpolarized light gives access to the surface magnetic field (H_s), which is the average magnitude of the field over the visible hemisphere. The H_s value is then deduced from the displacement observed on classical spectra. It is difficult to measure and very often the Zeeman pattern of the lines are not resolved in stellar spectra.

It is a pity, because H_s values are more representative of the magnetic energy and less sensitive to the field geometry than H_{eff} values. And H_s is

certainly more suitable to study the influence of the magnetic field on other stellar characteristics (rotation, abundances, . . .), or the correlation with parameters of interest in CP stars (photometric index of peculiarity for example). Moreover, the knowledge of H_s variation, in addition to that of H_{eff} , is necessary to get a better idea of the field geometry.

2. Method and Data for Surface Magnetic Field Measurements

As said above, the displacement of the magnetic component is very small and Resolved Zeeman Pattern (RZP) can be observed only in the most favourable cases, at least in slowly rotating stars ($V_{\text{sin}i} < 10-20 \text{ km/s}$). Although CP stars rotate more slowly than main-sequence stars of the same spectral type, the sample where H_s can be measured directly from resolved splitting is limited.

Few CP stars (34) have been measured for H_s , among them only 12 show RZP (Didelon, 1983). Extensive H_s measurements along the whole period of variation are available for only 4 stars (Landstreet, 1980).

In order to go further and to measure H_s in a greater sample, the differential broadening due to magnetic field, must be studied. The first attempt to compare the widths of lines with different Landé factors was done by Preston (1971). More accurate analyses must compare similar lines which are formed under the same atmospheric conditions and have approximately the same strengths. So

the lines must, if possible, belong to the same multiplet or super-multiplet, and must have approximately the same oscillator strength.

Several studies of that kind, more or less derived from the so-called "Robinson method" (Robinson, 1980), were undertaken, but have been applied to cool stars only. In fact, all these approaches used the comparison and/or the deconvolution of magnetic sensitive lines by magnetic null lines or lines less sensitive to the magnetic field (smaller z value).

One kind of procedure directly fits the profile of the magnetic line with 3 components. The parameters of these components are partially derived from the insensitive lines (Marcy, 1984). Then the "deconvolution" is done iteratively and finally gives the field strength and the filling factor, which is the surface proportion covered by the field.

Other procedures study the division of the Fourier Transforms (FT hereafter) of the two lines with different magnetic sensitivity (Sun et al., 1987 and references therein; Gray, 1984). The FT of a sensitive line is given by:

$$Pz(\sigma) = P_0(\sigma) * (1 - A + A \cos(2\pi n \sigma_0 \Delta)) \quad (2)$$

- $P_0(\sigma)$ is the FT of a magnetic null line,
- A is a function of the mean orientation of the magnetic field θ , and of the filling factor F : $A = 0.5 F (1 + \cos^2 \theta)$,
- Δ is the usual displacement of the components given by expression (1),
- σ_0 is the smallest frequency obtained in the FT, which corresponds to the length of the spectrum analysed,
- n is an integer which gives the different frequencies of the discrete FT.

The division of two FT eliminates $P_0(\sigma)$ and the Zeeman signature corresponding to the Zeeman broadening is obtained. If the division is made by the

FT of a magnetic null line, the theoretical Zeeman broadening function which must be used to fit the observational Zeeman broadening function is reduced to a simple form:

$$Z(\sigma) = 1 - A + A \cos(2\pi n \sigma_0 \Delta)$$

Both methods use the same assumptions and seem to have the same limitations. They assume that the magnetic field is homogeneous on the visible hemisphere, that the Zeeman pattern can be analysed as a triplet, and they suppose that the lines are unblended. However, several attempts have been made to study the influences of these shortcomings (Gray, 1984; Gondoin et al., 1985).

It would be of interest to test the application of the different methods to CP stars, and to check if the magnetic field values can be derived in rapidly rotating magnetic stars. In that way, slowly rotating magnetic stars must be studied first to see if the different methods are consistent and reliable.

Surface magnetic field measurements with both methods require high resolution spectroscopy with high signal-to-noise ratio. In fact, one must be able to see Resolved Zeeman Pattern (RZP) in faint lines or make a fine profile analysis of lines with different Landé factors. The unique combination of the CES and Reticon at the CAT allows to obtain such data.

During two observing runs at this instrument, in December 1985 and October 1986, I observed several CP stars at several different wavelengths. I want to present here the first results concerning the very slow rotating CP star HD 187474, of the Si-Cr-Eu type. It has a rotational period of approximately 7 years, and is therefore a very good candidate to perform the first tests.

3. Some Difficulties in Surface Magnetic Field Measurements

It is obvious that people involved in H_s measurements try to observe lines with the greatest Landé factors possible, and which at the same time have a Zeeman pattern as simple as possible. I want to mention here some patterns of interest. The quasi triplet pattern occurs when the groups of π and σ components are widely separated. Otherwise, if π and σ components are blended together, the g_{eff} values listed in Beckers (1969) cannot be used, but taking into account the complete pattern and considering the magnetic subcomponents involved in the observed splitting, z can be calculated. Another interesting case is the doublet pattern; it is a special case of the quadruplet pattern. It occurs when the two groups of π components have the same displacement as the σ component groups. Then only two components are observed and they are more easily resolved than 3 or several components with the same z . As already seen above, complicated patterns will be difficult to analyse. This is illustrated in Figure 1, which shows a doublet pattern observed in a FeII line of HD 187474 (the most simple pattern), and at the left of this line a very complicated structure. This feature is due to 2 nearby SiII lines with complicated Zeeman pattern, and possible additional blends with other faint lines.

It is also important to observe unsaturated lines. Otherwise, if they are too strong, they will be collisionally broadened, and information on the magnetic broadening will be more difficult to extract.

Moreover, as shown by expression (1), the displacement is related with the square of the central wavelength, and the splitting is more effective towards long wavelengths. That explains why people try to find suitable lines or line pairs in the red or even infrared region. But the choice is then limited by other constraints due to the earth's atmosphere. In fact, telluric lines of oxygen, water vapour or other species pollute large spectral regions which are then unsuitable for good measurements. For example a line pair of FeII (73) at 7223 Å which would be very suitable for Differential Magnetic Broadening (DMB) study is disturbed by a forest of strong lines of atmospheric water vapour.

It therefore appears that the selection of lines to be studied is very important and very difficult. The choice is also important because the Reticon length limits the wavelength range available for each exposure to 50 Å.

This choice is not made easier by the great differences in abundance patterns

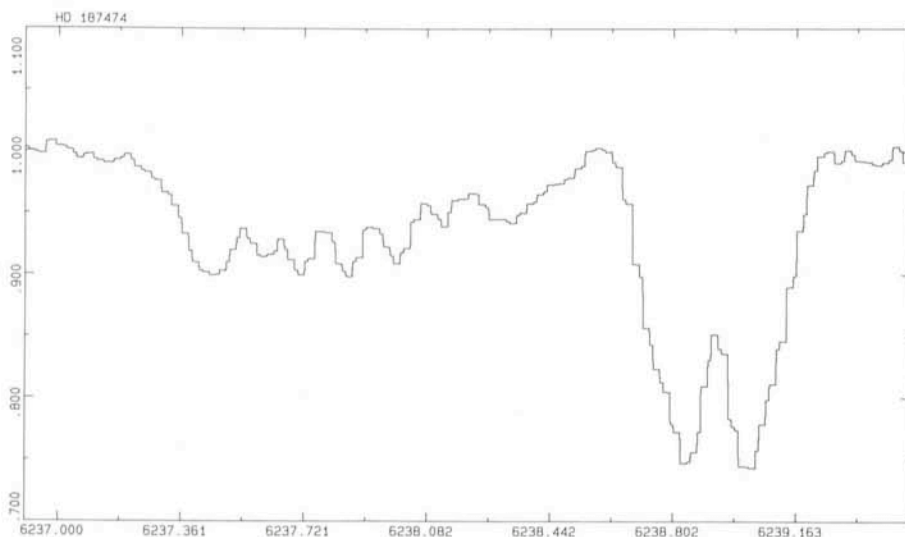


Figure 1: This spectral region of HD 187474 shows a doublet pattern in a FeII line and a very complicated structure due to simultaneous Zeeman splitting and blends of several lines.

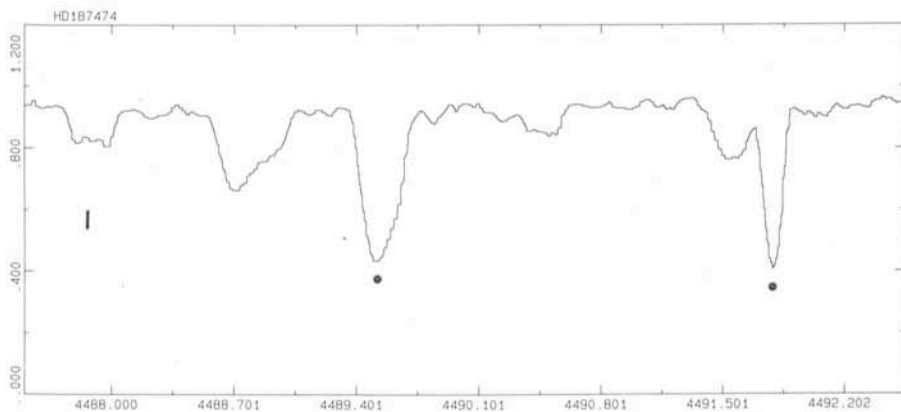


Figure 2: A portion of a Reticon spectrum of HD 187474. The points indicate two lines of Fe II with different magnetic sensitivity. Note their different widths. The bar indicates a resolved Zeeman triplet in a Cr II line.

encountered in CP stars. A strong, saturated line in one star, may be faint enough to be used, or may even disappear completely in other stars. Thus the choice depends not only on the lines themselves, but also partly on the selected stars to study.

Finally, I chose several spectral regions, in which lines with great z are present and can be observed in CP stars, and other regions with suitable line pairs for DMB analysis. The two lines of the pair must be located in the same 50 Å region, so they can be observed simultaneously with the Reticon.

All the problems mentioned above explain why clear RZP were usually not observed in the expected lines, but rather in unexpected faint lines (certainly with large z value) which appear in the chosen regions.

Another difficulty came from the line identification, but also from recognition and collection of the configuration, the Zeeman pattern and the z value.

The line identification in CP stars is not a trivial problem, even for strong lines (that is, those which are visible on photographic plates at high resolution 1–10 Å/mm, $W\lambda > 50$ mÅ). Such spectra of CP stars show unusual lines; lines from rare and heavy elements, or unidentified lines of common elements (i. e. Cr, Fe, . . .), usually not seen in normal stars. Even these strong lines are often not well studied in laboratory analysis, and atomic data are missing. The situation is worse at long wavelengths where atomic data are more likely to be missing.

In that way, the identification of faint (to very faint) lines detected in high resolution spectra with high S/N is a difficulty of first order. Moreover, the comparison of the strength or the presence of lines within a multiplet is not always possible due to the limited spectral range of 50 Å.

I want to point out that the lines analysed must be free of blends and must

be as clean as possible, at least to perform DMB studies. It is obvious then that line identification is unavoidable for the best part, and that the choice of stars to be observed becomes more and more difficult. In fact, it is tempting to observe cool CP stars with strong overabundances. They would have many lines and the probability to see unexpected RZP is increased, but at the same time, blends will occur more often. This probability is also increased when the rotational velocity increases, due to the resulting line broadening.

All the above considerations show that the choices of the lines and of the stars to be observed are not independent. It is even more difficult to predict with certainty which lines will be suitable because the available atomic data are neither complete nor precise, even for common ions like Cr II, Ti II, . . . Only the observed spectra will show if the right choices have been made, and the experience will certainly bring up some useful and suitable lines or regions.

4. The Surface Magnetic Field of HD 187474 from RZP Study

In order to test and to compare the different methods of H_s measurement, the H_s first has to be determined from

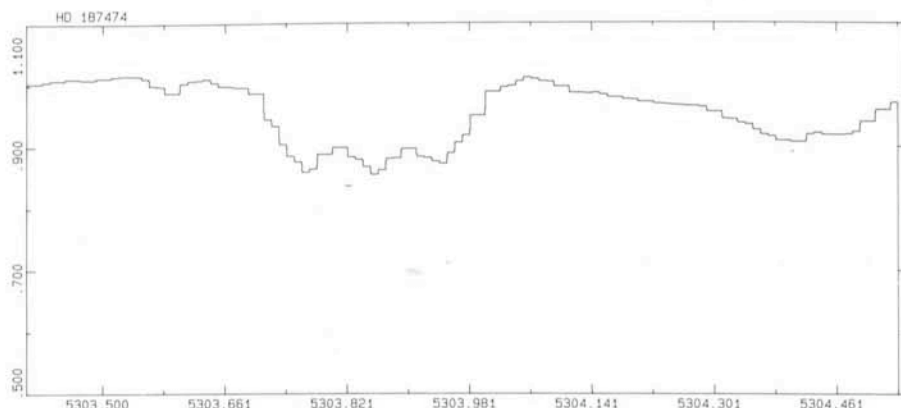


Figure 3: Resolved triplet observed in a Fe II line.

RZP, if possible. Five Reticon spectra of HD 187474 were obtained in October 1986. They cover the following wavelength regions: $\lambda\lambda$ 4488–4523, $\lambda\lambda$ 5000–5040, $\lambda\lambda$ 5274–5314, $\lambda\lambda$ 6214–6265, $\lambda\lambda$ 7373–7426.

First of all, it is interesting to check by visual inspection if the H_s influence on the line profiles is noticeable. From the above-mentioned limitations and difficulties, it is obvious that DMB effects are certainly not easy to detect and analyse in some stars. However, effects are clearly visible in HD 187474. This is certainly due to the low rotational velocity and therefore the sharpness of the lines. This is illustrated in Figure 2 which reproduces a part of the spectrum in the lowest wavelength range. This range was chosen because it covers a region where 4 Fe II lines of the same multiplet (No. 37) are present. Moreover, they have approximately the same intensity but have different z values. Two of them are seen at 4489.5 Å and 4491.8 Å in Figure 2. Their z values are 1.5 and 0.4, respectively. The width difference is the signature of the DMB effect. A small blend is perhaps present in the red wing of the magnetic sensitive line. To the left in the same figure, a RZP is present. This triplet can be attributed to a Cr II line. This line has the same Landé factor (1.5) as the Fe II line at λ 4489.5. That one does not show a RZP, certainly because it is too strong ($W\lambda = 0.127$ Å). This illustrates well the difficulty and the chance, which occurs in RZP observation, as stressed above. Two small and broad lines (certainly with high z values) are present at λ 4490.5 and λ 4491.5. The first one is definitely a Mn I line, but the second one cannot be identified with certainty. A broad blend of Ti II and Gd II is visible at λ 4488.7. Finally, this figure also gives an idea of the high S/N commonly obtained with the Reticon.

After this qualitative and visual check, the strength of H_s must be deduced from the observed RZP. But, as stressed above, RZP is seen mainly in faint lines that have to be identified.

TABLE 1: Resolved Zeeman pattern and Hs measurements

λ obs.	ion identification	z	$\Delta\lambda$	B
4487.90	CrII (63)	1.5	.078	5.5
4502.61	MnI (22)	1.5	.065	4.6
4521.68	GdII (44)	1.91	.0985	5.4
4522.34	GdII (135)	1.19	.056	4.9
5011.80	?		.048	
5303.86	FeII (225)	1.14	.0815	5.5
5306.34	CrII (24)	1.63	.0845	3.95
6221.56	?		.122	
6227.17	CrII (a)	0.6	.054	5.0
	(105) (b)	1.8	.1525	4.7
6232.24	AlII (10)	1.0	.109	6.0
6238.93	FeII (74)	1.11	.10	4.97
6241.48	?		.130	
6243.67	AlII (10)	1.17	.1285	6.05
6249.02	?		.117	
6249.40	FeII Lund	1.5	.125	4.6
7420.32	?		.0955	

(a): case of the π components
 (b): case of the σ components
 "Lund" means that the identification comes from Johansson (1978) table.

I tried first to identify all the "strong" lines (residual intensity < 0.7) visible in the spectra. I used for this purpose the Moore table (1945) and the NBS table (Reader and Corliss, 1982). Moreover, for FeII, I used the line list prepared by Johansson (1978). The Moore table gives the configuration and then I can deduce the z value from Beckers table (1969). However, the NBS table does not give the configuration and then the identification is not useful for the study of Hs effects.

Once the identification of the strong line had been done, I selected the most "beautiful" and clear RZP. When the identification was possible I deduced from the observed $\Delta\lambda$ a value for Hs. All these data are listed in Table 1. The magnetic field strength is given in kilogauss, and the displacement $\Delta\lambda$ in Å.

Figure 3 shows a typical triplet observed at λ 5303.8, which is due to a

high excitation line of FeII (multiplet No. 225, z = 1.135).

Figure 4 shows an unusual RZP. This quadruplet is due to CrII (105). In this case it is possible to calculate an Hs value from the displacement of the σ components as usually, but also from π components. The two values are close together.

With the doublet pattern shown in Figure 1, the landscape of possible Zeeman pattern is well illustrated.

Now let us see what is the mean of the Hs strength. In Table 1, 16 RZP are listed, 5 have not yet been identified and 12 values of Hs can be calculated. They range from 3.95 to 6.05 kgauss, the mean value is 5.1 and the dispersion 0.6 kgauss.

The distribution of the Hs values are approximately the same for the different elements. So, if there is a patchy distribution of the element overabundances on the stellar surface, it does not

greatly affect the Hs measurements. However, almost all the elements listed in Table 1 belong to the group of the iron peak or to the rare earths. They should have the same distribution and no differences are expected. The only different element (AlII) gives a slightly greater field (see below). Its distribution on the surface is perhaps not identical.

I want to point out that on the one hand the smallest value is very different from others, and does not fit the distribution very well. It is certainly due to a wrong measurement of the resolved pattern, which is not well defined, or to a bad z value. On the other hand, the two largest values (6., 6.05) came from the 2 AlII lines. If we eliminate these 3 values the distribution is restricted to the 4.6–5.5 domain. The mean does not change at all and the dispersion is only slightly reduced,

$$H_s = 5.0 \pm 0.4 \text{ kgauss.}$$

This is the first value of the surface field available for HD 187474. It should be compared to the Hs value of 2.3 kgauss deduced from the Geneva photometry. The disagreement is important and questions the validity of the relation established before (Cramer and Maeder, 1980; Didelon, 1984). Though the Hs value is close to the application limit of the relation, a better agreement would have been expected.

The good quality of the data allows not only to measure the displacement of the components, but also their individual intensities. This additional information will put some constraints on the field geometry (orientation). In fact the displacement is related to the field strength, but is not influenced by the geometry. On the contrary the intensities of the components are a function of the angle between the magnetic field orientation and the line of sight, but do not depend on the field strength. The relative intensities of the π and σ components are:

$$\begin{aligned} I_\pi &= a/2 \sin^2\theta \\ I_\sigma &= a/4 (1 + \cos^2\theta) \end{aligned}$$

Then the ratio of their intensities permits the determination of the mean magnetic field orientation.

Visual inspection of the resolved triplet shows that π and σ components have approximately the same intensities. The measurements of their equivalent widths give the following ratio: $I_\pi/I_\sigma = 0.98 \pm 0.2$, which corresponds to $\theta = 55^\circ \pm 5^\circ$.

This angle is more or less related to γ , the inclination of the magnetic axis to the line of sight. It depends on the field geometry, but for dipolar field they are closely related.

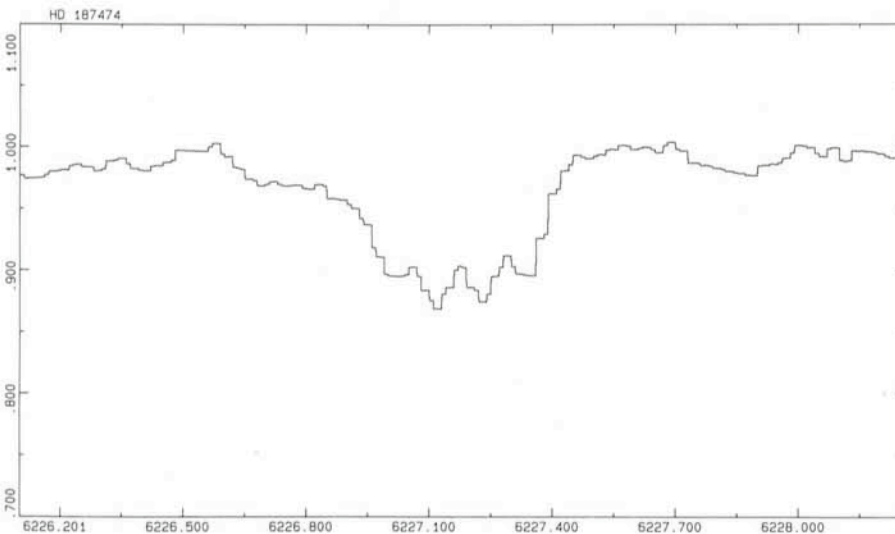


Figure 4: Resolved quadruplet observed in a CrII line.

In conclusion, the high quality of the data obtained with the CES and the Reticon allowed to make a fine analysis of the RZP observed in the slow rotation star HD 187474. So, the strength of H_s and its mean orientation were derived. This is one of the rare cases where the orientation of the magnetic field was possible.

I want to point out that it would be of great interest to follow HD 187474 during the whole period. On the one hand it will allow to determine the H_s variation and hence, put some constraints on the field geometry. If the inclination determination is possible at all the phases, it will also contribute to the study of the geometry. On the other hand, if the H_s variation is big enough it would be a good occasion to test the different methods of H_s measurement in slowly rotating stars and eventually determine their limitations towards small fields.

5. Differential Magnetic Broadening and Fourier Deconvolution

The strength of the field and its mean orientation can also be determined from the study of DMB effects. It is interesting to check if the Zeeman signature (also called Zeeman broadening function) can be described with the values determined above from RZP. The Zeeman Broadening Function (ZBF hereafter) is obtained by the division of the FT of two lines with different z values.

It is not obvious whether the Robinson method can be applied to CP stars. In fact, it has been developed to describe and study the magnetic field of late-type stars, which have a quite different field, similar to the solar one. The main problem arises from Doppler shift due to stellar rotation. Its combination with the surface field distribution on the visible hemisphere will distort the line profile. Then the magnetic effects would be more difficult to analyse. However, for slow rotating stars, like HD 187474, this difficulty is removed, and a test can be performed with good confidence.

I studied the DMB effects on Fe I lines present in the first wavelength range. I used the line at λ 4491 Å ($z = 0.4$) as an insensitive magnetic line of reference. The three other lines have greater z values and are more sensitive to Zeeman broadening. Their wavelengths and z values are respectively; λ 4491 Å, $z = 1.5$; λ 4515 Å, $z = 1.0$; λ 4520 Å, $z = 1.5$. The division of the FT of one of these three lines by the FT of the "insensitive" reference line gives the observational ZBF to be compared to the theoretical ones. The equivalent widths of these lines are not equal. The lines with large z are stronger than the line with $z = 0.4$. To compare "identical"

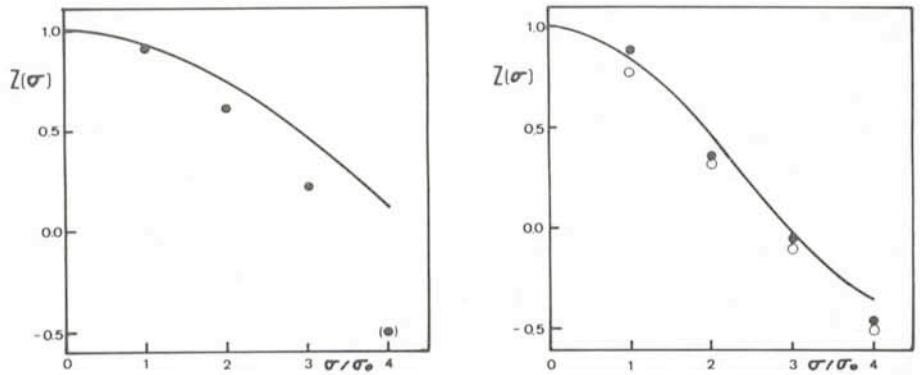


Figure 5: Zeeman broadening functions associated with different magnetic sensitive Fe I lines and the insensitive Fe I line (λ 4491, $z = 0.4$). The full lines give the functions calculated with the parameters deduced from resolved Zeeman pattern ($B = 5$ kgauss, $A = 0.66$). (a) The dots represent the observed broadening function associated with the sensitive magnetic line λ 4515 ($z = 1.03$). (b) Observed broadening functions associated with the magnetic sensitive line λ 4520 (full dots) and λ 4489 (empty dots). The two lines have the same z value (1.5).

lines by the division of FT, I scaled the reference line to the strongest line. (Marcy, 1984).

The expression (2) is used to calculate the theoretical ZBF for each line pair. As I extracted a region of 0.63 Å to perform the FT of each line, the value of the smallest frequency σ_0 is given by 1.587 \AA^{-1} . The factor A is a function of θ , the mean orientation of the field, and F the filling factor. The θ value determined above is adopted (55°). The magnetic fields of CP stars cover the whole surface, so I assumed that F equals 1. Then the A value is 0.66. Δ is calculated for each line, taking for B the value of the field determined above (5 kgauss).

Figures 5a and 5b show the comparison of the observed and calculated ZBF. The full lines correspond to the calculated ZBF, with $A = 0.66$, the points give the observed ZBF. The ZBF obtained with the sensitive ($z = 1.03$) line λ 4515 is plotted in Figure 5a. In Figure 5b I plotted the ZBF obtained with the 2 other sensitive lines, which have the same z values (1.5). The observed ZBF of λ 4520, and λ 4489, are represented by dots and circles, respectively.

The large value of A gives a very sharp function. The ratio of Fourier amplitudes at high frequency is therefore small (see Figs. 1 and 2 in Gray 1984). The noise will be dominant and it will reduce the available points of the observational ZBF. Due to that limitation, only 4 points were useful in the data.

The agreement between the calculated and the observed ZBF of the lines with $z = 1.5$ is satisfactory (Fig. 5b). Moreover, the two observed ZBF have approximately the same values, which confirms the reliability of the data. The point of highest frequency ($\sigma/\sigma_0 = 4$) is a little bit off the curve. This is perhaps due to noise contamination, which appears already at that frequency. However, I try to better reproduce the obser-

vations. A best fit would be obtained with a greater A value or with a stronger field. In fact, the determination of A and B is not independent (Gray, 1984; Marcy, 1984). In the present case, I assumed that the magnetic field strength is well known, and to my point of view, the mean inclination determination is less satisfactory. A best fit would require approximately $A = 0.7$, which corresponds to $\theta = 51^\circ$. This value is still compatible with the adopted θ error.

The calculated ZBF of the line λ 4515 ($z = 1.03$) did not fit the observed one, which is much steeper. A better agreement would require at least $A = 0.9$ and so $\theta = 26^\circ$. This value is no more compatible with the inclination deduced from RZP. This effect is due to additional broadening of the line and the most probable explanation is the contamination by a small undetected blend.

I observed another line pair of Fe I at λ 7400 Å, suitable for DMB study. But the lines were too faint and the spectra too noisy for that purpose. So the ZBF of that pair cannot be used.

Finally, for the 2 lines with $z = 1.5$, a good agreement exists between the observational ZBF and the ZBF calculated with the values determined from RZP analysis. That shows that the Robinson method can certainly be used to determine H_s , at least in slowly rotating CP stars. Because even if they do not show RZP, it is possible to measure H_s . However, careful attention is required to choose suitable line pairs. Moreover, at least several ZBF are necessary to get a field value with a good confidence level and to avoid undetected additional sources of broadening or inaccurate atomic data.

6. Conclusion

A more extensive study, taking into account all the observed resolved Zee-

man patterns, will be published later. I also plan to pursue the tests of the "Robinson" method and other methods of H α measurements.

This preliminary study of Resolved Zeeman Pattern allowed the determination of the surface magnetic field strength of HD 187474, and its mean inclination on the line of sight at the time of observation.

Moreover, the comparison of observed and calculated Zeeman broadening functions shows that the "Robinson" method will be suitable to

measure the surface magnetic field, at least in slowly rotating CP stars.

References

Beckers, J.M.: 1969, Table of Zeeman Multiplets, *Physical sciences research paper*, No. 371.
 Gramer, N., and Maeder, A.: 1980, *Astron. Astrophys. Suppl. Ser.* **41**, 111.
 Didelon, P.: 1983, *Astron. Astrophys. Suppl. Ser.* **53**, 19.
 Didelon, P.: 1984, *Astron. Astrophys. Suppl. Ser.* **55**, 69.
 Gondoin, Ph., Giampapa, M.S., and Bookbinder, J.A.: 1985, *Ap. J.* **297**, 710.

Gray, D.F.: 1984, *Ap. J.* **277**, 640.
 Johansson, S.: 1978, Lund preprint, to be published in *Physica Scripta*.
 Landstreet, J.D.: 1980, *A. J.* **85**, 611.
 Marcy, G.W.: 1984, *Ap. J.* **276**, 286.
 Moore, C.E.: 1945, A Multiplet Table, NBS Tech. Note No. 36.
 Preston, G.W.: 1971, *Ap. J.* **164**, 309.
 Preston, G.W.: 1974, *Ann. Rev. Astr. Astrophys.* **12**, 257.
 Reader, J. and Corliss, C.H.: 1982, *CRC Handbook of Chemistry and Physics*, E204.
 Robinson, R.D.: 1980, *Ap. J.* **239**, 961.
 Sun, W.H., Giampapa, M.S. and Worden, S.P.: 1987, *Ap. J.* **312**, 930.

The Clouds which Form the Extended Emission Line Region of NGC 4388

L. COLINA, *Universitäts-Sternwarte, Göttingen, F.R. Germany*

Introduction

Since the discovery of Seyfert galaxies (Seyfert, 1943) and Quasars (Schmidt, 1963) most of the attention to these active galaxies has been directed towards understanding the physics of the nuclear non-thermal source, the structure of the inner emission line regions, (the so-called *Broad Line Region*), where the observed broad and variable emission lines are produced, and the coupling between both phenomena.

Further out, there exist extended emission-line regions with sizes up to a few kpc and where the observed strong optical, narrow forbidden lines are formed. These regions, usually called *Narrow Line Regions*, are considered as the link between the nuclear regions and the outer interstellar medium.

Work by Heckman and collaborators (Heckman et al., 1981) and subsequently by Whittle (Whittle, 1985a, b) showed the presence of a blue asymmetry as a general feature of the spatially unresolved [OIII] λ 5007 Å line profile in Seyfert galaxies. This characteristic, not observed in the HII and starburst galaxies, was interpreted as a consequence of peculiar motions in the central regions of these active galaxies. Models considering outflowing emission clouds embedded in a dusty medium, i.e. the receding clouds being preferentially obscured, or infalling dusty clouds, producing the opposite effect, most likely explain these observations.

Direct correlations between the line width of the spatially unresolved narrow emission lines and the ionization potential or the critical density have been observed in Seyfert galaxies (De Robertis and Osterbrock, 1984, 1986). This indi-

cates some kind of stratification in the physical conditions present in these regions, and covering a range which extends continuously from the Broad Line Region, $N_e \approx 10^9 \text{ cm}^{-3}$, through the Narrow Line Region, $N_e \geq 10^3 \text{ cm}^{-3}$.

Spatially resolved spectroscopic observations of the extended emission line regions in nearby Seyfert galaxies are crucial to understand how the physical, kinematical and ionizing structure of these regions evolve as a function of distance from the nucleus and position within the galaxy, how their structure is affected by the presence of the nonthermal nuclear source and which is the role of the interstellar medium.

Observations

Observations of NGC 4388 have been done at the Cassegrain focus of the La Silla 2.2-m telescope using the ESA Photon Counting System, the scientific model of the Faint Object Camera (see di Serego et al., 1985 for a detailed description). In the spectroscopic mode, the ESA PCD uses an array of $1,024 \times 256$ pixels (spectral \times spatial direction) with a pixel size of 25 μm . The slit width was 1.5 arcsec and the scale along the slit was 1 *arcsec* \cdot *pixel*⁻¹ giving a total length of the slit of 256 arcsec on the sky.

Long-slit spectroscopy covered the spectral range [OIII] $\lambda\lambda$ 4959, 5007 Å + H β at 21 Å/mm giving an effective resolution of 56 $\text{km} \cdot \text{s}^{-1}$ (FWHM at λ 5000 Å). Typical exposure times were 40 minutes divided into two periods of 20 minutes each. To monitor the geometrical distortion and to make the final wavelength calibration, HeAr com-

parison spectra were obtained after each single exposure. The observations in the various slit positions were optimized with respect to the position of the object on the sky in order to minimize the differential refraction effects. Finally, in each two dimensional spectrum, the signals of three adjacent spatial pixels were combined to increase the S/N ratio and to take into account the seeing effects.

Discussion

NGC 4388 is a highly inclined spiral galaxy located at the core of the Virgo cluster and classified as Seyfert 2 galaxy. Long-slit spectroscopy was obtained at position angles 23° and 152°. The slit at 23° was positioned to cover the direction at which a radio emission region extending over 40 arcsec was previously reported (Hummel et al., 1983). Emission on the [OIII] lines was observed over a total extension of 24 arcsec symmetric to the nucleus.

Contrary to the general behaviour observed in the [OIII] line profile of Seyfert galaxies, NGC 4388 shows a peculiar red-asymmetry (Fig. 1). The overall [OIII] λ 5007 Å line profile is composed, both at P.A. 23° and P.A. 152°, of five clearly distinguishable components, separated by up to 600 $\text{km} \cdot \text{s}^{-1}$ (see Table 1). The main component, C₂, extends over the central region from 3 arcsec NE to 6 arcsec SE. The other two major components, C₃ and C₄, appear to extend over a region of ± 6 arcsec symmetrically with respect to the nucleus. Finally, the smaller components, C₁ and C₅, are concentrated at the centre. These components could be